

AEROELASTIC RESPONSE OF CHORDWISE FLEXIBLE WINGS SUBJECTED TO GUSTS: AN INITIAL STUDY ON EXPERIMENTAL AND COMPUTATIONAL VALIDATION

J. Worotynska^{*,†}, G.A. Vio^{*,‡}

^{*}School of Aerospace, Mechanical and Mechatronic Engineering, The University of Sydney, Sydney NSW 2006, Australia

[†]jwor6083@uni.sydney.edu.au; [‡]garth.vio@sydney.edu.au

Keywords: *aeroelasticity, wind tunnel test, flexible airfoils*

Abstract

This paper sets up the experimental procedure for validating an analytical solution for the aeroelastic response of a chordwise flexible aerofoil under gust excitation. The design approach and limitation of the experimental set-up will be highlighted and the consequences in validating a theoretical model. A variety of designs approaches for a flexible wing are presented and the work which was done in support of the designs. The constraints imposed by the wind tunnel on the construction of the experimental test rig are outlined as well as the design of the gust generation device. The methodology, including the data collection devices and their functionality, is established. Future work is also suggested.

1 Introduction

As new aircraft become lighter and their wings more slender, the aircraft performance improves but they in turn become more flexible, making them more susceptible to gust loading [1]. When designing aircraft, aeroelasticity plays a part in maximising efficiency and durability especially in such aircraft as UAV's and long endurance aircraft. These vehicles present wings that are highly flexible, meaning they can no longer be assumed to be rigid in the chordwise direction [2]. Dowell presents aeroelasticity as involving the interaction of inertial, elastic and aerodynamic

forces and the phenomena which result from their interaction [3]. The interactions can be stable or unstable, and when testing aircraft designs, the goal is to determine whether any unstable aeroelastic phenomena could occur within the flight envelope.

The use of morphing technologies, where the structure can adapt itself to different flight regimes [4], requires the generation of accurate modelling in order to predict its aeroelastic behaviour. These structures allow for considerable changes in camber, hence the flexibility of the wing along its chord. Numerous studies have been performed on this subject to accurately model the aeroelastic effects. Different aerodynamic fidelity models have been employed to achieve this [5, 6], as well as linear/non-linear structures [7]. An overview of the current research is presented in a review paper by Shyy et al.[8].

A new low-fidelity modelling technique to account for gust loading on flexible aerofoils has been developed [9] for small scale UAV models undergoing linear deformations in the chordwise direction. However, whenever any such code is developed, validation becomes a prime consideration before it can be used for practical applications. The aim of this paper is to provide an initial framework for the experimentation required in order to validate such model.

2 Experimental Validation

2.1 Concepts

The experimental validation requires a variable stiffness model, a wing tunnel mount allowing a degree of freedom in both pitch and plunge, a method of gust generation, and equipment to measure the freestream velocity and wing deflection at various chordwise points. There were various design concepts discussed. The limitations of using a 3D wing to approximate 2D wing characteristics are that the tip vortices influence the lift generated. The gravitational effect on a horizontally placed wing would also influence the displacement of the model, thus the placement of wing has significance. Also, maintaining a camber while allowing sufficient chordwise flexibility to detect deflections requires a careful trade-off between the two. To remove the effect of tip vortices on the wing, the span of the wing is that of the wind tunnel. Gravitational effects can be negated through a vertical positioning on the entire setup. However the chordwise flexible wing of a specified camber still had a number of issues to consider. The concepts all revolved around the idea that multiple rigid elements were required in the spanwise direction. This maintained that every point at a chordwise distance behaved as closely as possible to all others at the same chordwise positioning. Since the theoretical code uses Thin Aerofoil Theory, the main approaches of maintaining a specified camber would be to:

- have the conventional wing cross-section by which the vortex distribution is estimated, or
- to actually have a thin wing whose cross-section was just the camber, thus more closely aligning the design with the code theory.

Using the conventional cross-section would require elements suspended at the required camber locations. This approach would require multiple elements whose interaction during wind tunnel testing and transportation could be precarious.

In addition, the complexity added to the model moves it further away from the analytical case. A simpler model design was sought which would be thin and follow the camber of the wing. A model with just a skin and stiffeners attached below that skin was considered, generating the desired lift for a wing with that camber. A modification of this design would be to apply a skin to all sides of the wing. A lattice structure within the wing would be very much like that generated in a finite element package like NASTRAN [10], thus the approach to validation would be more unified across the experimental and computational cases. The three design options considered were: a lattice structure, a curved plate simulating a camberline covered in a skin [8] and a curved plate on its own. The first solution was difficult to manufacture given the limited access to the necessary welding equipment. The second solution was constructed but found to be non-representative of the aerofoil as the skin had a tendency of overly flexing and changing the shape. The curved plate was the final solution used and is discussed further.

2.2 Design of Rig for Tunnel

This section outlines the design and feasibility of implementing a gust generation device into the research wind tunnel of the Defence Science and Technology Organisation's (DSTO). Discussions with the wind tunnel operators brought about multiple gust-generation options, the most feasible of which were jet streams and moving aerofoils. However on inspection of the wind-tunnel, jet streams did not seem apt for the tunnel configuration. The jet streams would potentially require modification of the tunnel which would be highly impractical given the low level of controllability.

It is undesirable for the gust-generating aerofoils to leave a wake, thus various aerofoil shapes were investigated to minimise the wakes created. This was mainly found through a minimisation of theoretical drag. Experiments performed in the 1960's [11] determined the aerodynamic characteristics of a NACA0012 aerofoil section for the range of Reynolds numbers from 1.44×10^6 to

2.88×10^6 . The decrease in pressure in the region of the wake is only 15% to 25% of the free-stream dynamic pressure. Symmetrical aerofoils, including the NACA0017, generally have very low wakes as can be seen by their low coefficients of drag. NACA0017 sections were readily available and were thus used for the gust mechanism prototype.

The rig for the wind tunnel was modelled in a CAD package to ensure that all the separately manufactured elements would fit together and within the tunnel provided, which is summarized in Figure 1. For the physical model see Figure 2. This was especially important given the short testing period of a week and the lack of physical access to the tunnel prior to testing.

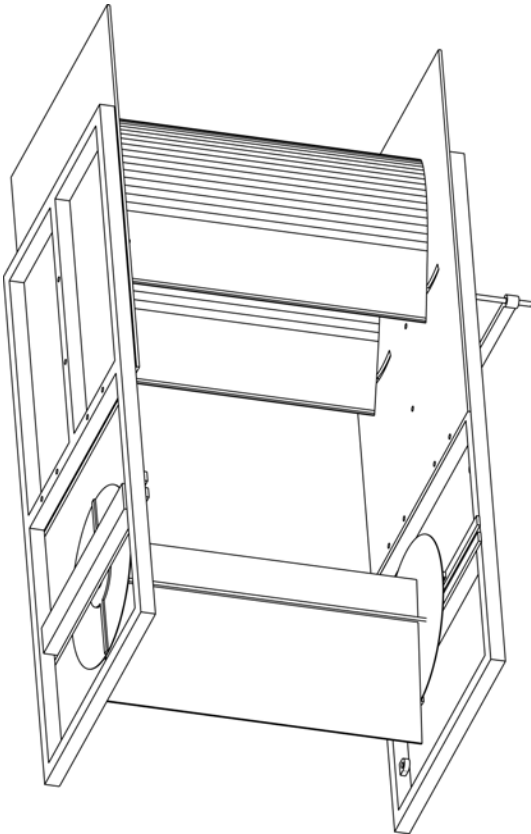


Fig. 1 The 3D model of the completed assembly as was to be manufactured.

The design was developed incrementally. The main features of the analytical model which were to be mimicked by the experimental rig were the two degrees of freedom, in pitch and plunge, and this was achieved using the rail sys-



Fig. 2 The experimental rig without the bottom frame.

tem which was developed. Each rail had a bearing enclosed which allowed for rotation about a pivot point but allowed only one direction of translational motion. The surface of the two plastics in this bearing is very much like Teflon, in terms of a low coefficient of friction, and as such, lubricant was not to be used as it could damage the material. This approach did have its limitations, as there would still be small amounts of freedom in the other directions, but overall the degrees of freedom would be much the same of the analytical model.

While the test wings would be able to move in pitch and plunge, their motion would not be totally free, but stiffened using springs, such that the wing would mimic the typical aeroelastic model. In the typical model there is a torsional and a translational spring attached. In the conceived rig, to limit the heave there would be two translational springs along the same axis attached to the axis with the main spar, see Figure 3. The two springs have the same spring constant and have the same initial displacement so that the heave motion is linear.

Rather than having a torsional spring in the rig, as in the typical model, two translational springs attached at an equidistant radius from the spar would provide opposing force during rotation. These springs were attached to the end plate to avoid non-linear effects, see Figure 4. The properties of the springs were evaluated experimentally and their stiffness are given in section 6.

The flow through the tunnel, given no gust



Fig. 3 The translational springs are limited in their direction of movement by the rail system.

input, would be fairly consistent, meaning the load distributed over the test wing would be constant along each point spanwise. The frame at the top and bottom of the tunnel, while important to space out the test and gust wings, would cause turbulence every time a part of the boundary was hit. As such, where possible a pseudo tunnel wall is placed in the form of a blocking board. This board has multiple features, despite its simplicity. The close alignment of the ends of the gust wings with the board results in minimal turbulence due to recirculation at the tips, much like the end plates for the test wings. The 200mm overhang forward of the frames means that some air would flow under the board and between the tunnel wall and hit the frame of the rig and this flow would subside. The remainder of

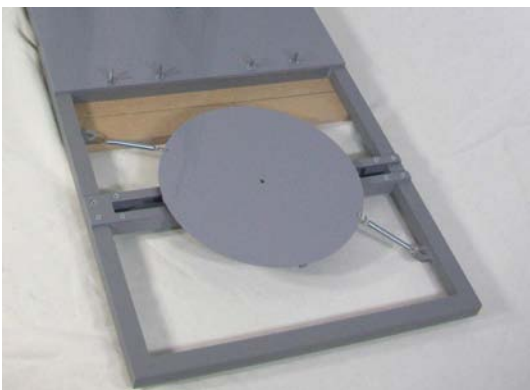


Fig. 4 Translational springs were attached to the end plate and offset from the pivot point to act similarly to torsional springs.

the flow would pass between the blocking boards and be much more laminar in nature than the turbulent flow which would have resulted without the boards. The bottom board also has slots cut such that the gust wings are able to rotate 15° direction from the centreline. Melbourne's paper [12] discusses the placement of the gust generating wings' offset from the test wing. The wings, while symmetrical with minimal drag, do produce a small wake, especially if imperfectly produced. Their presence also causes an element of blockage in the tunnel, thus placement of the test wing should minimise these effects. Essentially, the test wing should be experiencing close to freestream conditions as though the gust wings were not there, when the gust wings are along the centreline and unmoved.

The gust wings themselves slipped into openings in the blocking boards and frames and each had a rod which extended outside the tunnel through the slots cut open in the plywood panels. Each of these rods was slipped through a 'connecting rod' which allowed the gust wings to be moved in unison during the testing, see Figure 5.



Fig. 5 Gust generating wings are slotted into the blocking boards and their controlling rods pass through the slots at the bottom of the tunnel.

The motion of the top plate, limited by the 'heave' springs, could be mimicked by the bottom plate and the motion of the bottom plate, limited by the 'pitch' springs, could be mimicked by

the top plate, given the right physical limitations. That is, the rotation of the wing due to the oncoming air velocity but opposed by the 'pitch' springs would be the same at the top if the spar of the wing had a circular opening, meaning the wing would be free to copy the bottom motion at the top. However, the bottom end of the spar could not be circular, as this end of the wing would have to be locked into the bottom plate which limits it. Thus the bottom end of the spar was square and given a square hole into which it was inserted, such that the rotational motion of the wing and the resistance due to the springs was related. The test wings are meant to represent aerofoils, meaning to mimic two-dimensional aerodynamics, end plates are necessary so as not to have the recirculation at the tips of the wing. However, as the wing is meant to be flexible in the chordwise direction, connecting the end plates directly to the wing would impose a limitation in the chordwise motion. Two options were available: either the wings could be extremely long, thus at the midpoint of the span the motion would be approximately two dimensional, or small gaps would be placed between the end plates and the test wings, such that only a small amount of recirculation would occur. The latter option was chosen given the size restrictions of the tunnel. A 1 to 2mm gap between the endplates and the wings would cause a small amount of recirculation, allow for the flexibility of the test wings and fit into the 620mm height restriction of the tunnel. The properties and dimensions of the test wings are given in table 2 and 3. There were two options for the placement of the test wings within the tunnel: vertical or horizontal. While the width of the tunnel is greater at 800mm, meaning the recirculation would have a smaller effect than the placement of the wings vertically, the horizontal placement of the wing would cause the wing to sag in the middle due to gravity, thus causing greater aerodynamic problems due to the shape of the aerofoil. As such, the vertical placement was selected. The lift distribution along the chord also sees the majority of the force located closer to the leading edge. The further back the spar could be placed on the wing, the greater the moments ex-

perienced about the axis of the spar. Placement of the spar on the underside of the wing was on the basis that the top surface is most responsible for lift generation, and as such, placement of obstructions along this surface would disrupt the expected lift properties of the wing.



Fig. 6 The test wings slot into the end plates.



Fig. 7 The rotational point of the wing is at the spar which is placed closer to the leading edge than the trailing edge.

The gust wings had the NACA0017 cross-sections manufactured out of PVC plastic. The

test wings themselves were manufactured of two different plastics, Foamex and PETG, which gave them different inertial properties. Both were applied to a consistent NACA4212 aerofoil section which was approximated by the camberline, as with thin aerofoil theory. This meant that the differences in the results would be due to differences in the mass distribution rather than a difference in the aerofoil. The NACA4212 is the baseline test case used in the computational validation. Such a high camber also meant that the placement of the relatively thin spar at the quarter chord would have its drag affects minimised, as the flow would hit the leading edge prior to the spar. Certain elements of the design slot together, such as the gust and test wings into the frame, and others, such as the blocking boards and frames need to be bolted to the panels of the wind tunnel, to provide support for the weight and limit the vibrations experienced due to oncoming airflow. While most of the components of the set up were quite easily laser cut, turned and drilled, the test wings proved the most difficult to manufacture. A mould for the NACA4212 test wing was made and the plastic for each wing bent into shape with the use of an oven. However, during the process of bending and cooling, the plastics significantly shrunk. The simplest solution found was to start with a sizably larger piece of plastic, about twice the size, from the wing and then cut it down to size after it had cooled and stabilised.

2.3 Experimental Data Collected

The DSTO Wind Tunnel is an open-circuit continuous flow tunnel. In an empty test section it has a range between 5 and 30m/s. The test section is nominally 1020 mm long, Figure 9, and has a cross section of 400,000 mm square, Figure 8. The sidewalls are interchangeable and can be either solid or slotted.

The transparent panels that were present were utilized for the side walls. The top and bottom walls were made of plywood. The test conditions were set during the calibration day. The free stream velocity was varied between approximately 5 and 25 m/s, as blockage due to

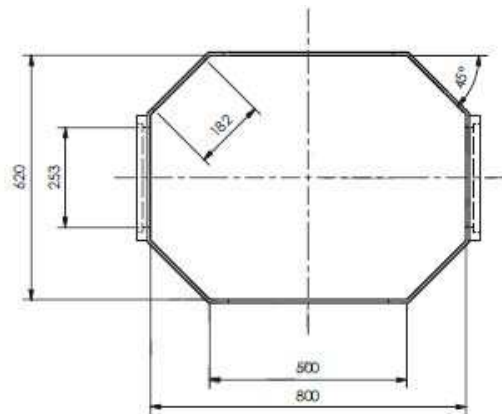


Fig. 8 Research tunnel cross-section

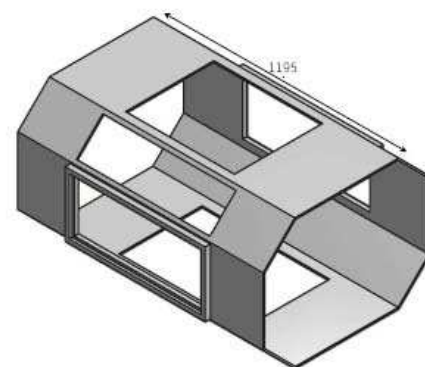


Fig. 9 Research tunnel test-section

the model prevented higher speeds, and the test wings were monitored to identify any significant decrease in stability. If excessive levels of vibration had been identified, the tests would have been stopped, and that velocity region would not have been approached again. This was, however, not the case with the two test wings used. Velocities were selected on the basis that all sensor readings were large enough to be distinguished from other sources of noise. Lower velocities were best for this sort of testing. A variety of gust inputs were tested using the manual rotation of the gust wings. From the preliminary observations, a high frequency sine wave input appeared to produce the greatest visible reaction by the sensors, and was the gust input used for the various test points. As the analytical code needed to be validated using a given gust input, the velocity at the leading edge of the test

wing had to be measured, which was achieved using a hot wire anemometer. The displacements were measured using six accelerometers evenly spaced along the chord of the wing at about the midspan. To ascertain that the test wing is in fact acting as a NACA4212 section, three Kulite pressure transducers were spaced on the top surface of the wing: at the leading and trailing edges as well as the quarter-chord. A Pitot tube was set up ahead of the test rig to measure the undisturbed free stream velocity. The six ICP accelerometers (PCB Piezotronics Model 352C22) were used and these were spaced evenly along the chordline. The locations are given in table 4. The accelerometers were attached to the inside of the lower surface on the midspan location of the model wing in the chordwise direction using beeswax..

The upper surface is instrumented with 3 Kulite transducers in the chordwise direction at the midspan of the model wing, at the leading edge, trailing edge and quarter chord. These transducers are Model LL-125-15A which have a range of 15 psi absolute (104 kPa).

Modal testing was performed using an impact hammer. A roving technique was used to study the modal characteristics of the test model and structure in order to evaluate damping and frequency for comparison with the analytical model. The acquisition system which was used was the LMS Data Acquisition system as both strain gauge and ICP channels were available, as well as comprehensive software for quick analysis on the fly. The calibration of the sensors was done using the LMS software, except for the hot wire anemometer which was calibrated externally each day of testing.

2.4 Results

The tunnel used was a suction tunnel, meaning that any holes in the walls would disturb the flow slightly by pulling in air from the surrounding atmosphere. The slots in the bottom panel of the tunnel, through which the rods to control the gust wings passed, did let some extra air into the tunnel. However, due to the relatively

small size of these slots when compared to the test section, the disruption to the flow was minimal. The bolts which were used to secure the frames in the tunnel had heads which were protruding into the test section and thus were once more disturbing the flow. Since the flow at the midsection was of most interest, the disturbance would have had a small effect. Nonetheless, in an attempt to minimize these effects, the bolts were placed towards the sides of the tunnel rather than directly in front of the test wing. If the holes for the bolts were countersunk this would improve the design. Tape was attached to hold down the accelerometer cables and pressure transducers would cause the airflow over this section to differ to that over the rest of the test wing. The tape was attached the entire length of the chord; if it were not the change from tape to plastic would have made separation more likely. In general the experimental rig behaved as predicted, with the test wing free to move in heave and pitch. The one improvement to be made to this is to have the translation springs also on the bottom frame and the torsional springs on the top frame, to limit the asymmetrical displacement of the test wing due to the difference in stiffness between the two ends. While this wasn't noticeable in the tests, it would make the model more valid as a pitch-plunge aerofoil and allow for testing at higher velocities where those effects would be more evident. In the future, sensors at various spanwise locations should be used to confirm the motion is the same along the span of the wing, thus verifying that the test wing is acting as a pitch-plunge aerofoil. Having displacement sensors off the test wing would also minimise the change in the wing properties (mass and damping) and reduce the increase in drag due to their presence. The accelerometers could potentially be replaced with a row of lasers to directly detect the displacement of the wing without the influences mentioned. The other option is to use motion capture by placing contrasting dots on the wing and replicating the motion using the appropriate software. While the dots would disturb the flow more than the laser solution, their influence would be less so than the accelerometers and pressure transducers

with their cables.

The hot-wire anemometer was placed at the leading edge of the test wing. However, when subjected to gusts, the signal was noisy, with no variation in input detected even after considerable filtering. The signal which was picked up by the hot-wire appeared to be due to the local vibration of the wing in the tunnel. Hence the Pitot tube, which was just ahead of the test wing, was used to detect the local change in pressure due to the gust input and the results were post-processed into a usable gust velocity. The gust velocity was very clear when using this method of detection. However, another Pitot tube should be placed ahead of that gust wing to have a point of comparison for the correct free-stream velocity..

The pressure transducers did detect the changes in pressure due to the gusts. The transducers also picked up the induced pressure by the wing vibration, as it was evident after processing the data, whereby the magnitude of the pressure coefficients along the wing was found to be too large. As the transducers use piezoelectric crystals, it would require the use of two transducers at each station to use in differential mode in order to accurately measure the pressure difference generated by the wing. As only a limited number of transducers were available, this solution was not possible to test.

The gust inputs were very consistent despite being a manual input. This was due to the limitations placed by the guiding slots in the bottom blocking board which allowed for 15° of movement in either direction from centre. These slots were also the reason there were trigger accelerometer spikes, as the rod used for motion hit the side wall and caused higher sudden loading detected by the accelerometer, see Figure 10. Twenty gust readings were taken for every run which allowed for a power spectral density to be recorded by the data acquisition system. However, for consistent inputs, a motor should drive the gust generating rods so that a power spectral density with a higher level of coherence can be achieved. The use of a motor could also guarantee a return of the gust wing positions to zero de-

flection, which was very difficult to achieve with the manual input and sometimes caused a disturbance to the freestream velocity prior to the new gust input.

Unlike the pressure transducers and the hot-wire anemometer, the purpose of the accelerometers was in fact to pick up the motion of the wing and, as such, the readings came out well; detecting the violent movements in response to the gust input. The accelerometer placed at the connecting rod for the movement of the wings was termed the ‘trigger accelerometer’ as the LMS data acquisition system would use this input to start a new sample of data collection. The spike in the trigger accelerometer loading is indicative of a gust input, and the subsequent higher g-loading of the other accelerometers around this time indicate a response.

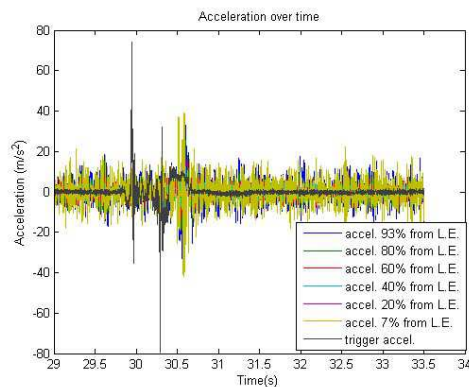


Fig. 10 Accelerometer readings over time, for run 2. The initiation of the gust is seen by the spike in the trigger accelerometer.

The results from the accelerometers were linearly integrated over small time intervals. As 2000 samples were collected per a second. The integration used the Trapezoidal Integration Method with an unknown constant of integration which caused drift in the signal when integrating. As this is constant, and it is known that once the transient response has subsided the wing returns to its initial position, that boundary condition was applied.

Figure 12 displays the displacement of each accelerometer over time. The dip in all the charted displacements at about 30.5s depicts the

near simultaneity in the movements of each accelerometer, and thus not an error in individual readings. The response of the trailing edge is seen to be the largest. This is as expected given this accelerometer has the largest moment arm in relation to the pivot point. The test conditions and main results for all of the test cases are displayed in Table 1.

A point to note is that the maximum displacement did not occur at the highest gust velocity but was related to a number of factors, including the gust velocity as a ratio of the freestream velocity. The maximum displacement in relation to the gust occurred at runs 2 and 5. This could be due to a greater response of a particular mode at the given conditions. The nonlinear relationship between the gust and the maximum displacement is depicted by the variation in the max displacement/gust ratio. For both test wings there was a higher amplitude response seen at about 33.7 to 34Hz and a harmonic response again at 67Hz using the power spectral density. Since the response was similar for both wings of different material properties, it was postulated that the responses were not of the wings themselves but of the surrounding experimental rig. Following the free-free body roving hammer modal testing it was found not to be so, and that the wings simply had similar frequency responses. The modal testing of wing 1 was conducted using a roving impact hammer technique. This saw the placement of an accelerometer at one corner of the wing and having the wing as a free-free body. Tapping the body on a matrix of points entered into the LMS data acquisition system, the frequency responses of the wing were recorded, see Figure 13.

While there were clearly higher order responses, only responses below 100Hz were really of interest, thus the observed range was limited between 0 and 100Hz, see Figure 14. Only lower order responses are of interest as these are the ones which tend to have the largest effect on the system.

Responses were seen at 6.5, 16.3, 21.8, 35.5, 52.3 and 65.3Hz. Theoretically the responses should be sharp, indicative of a specific frequency response, however, due to the flexibility

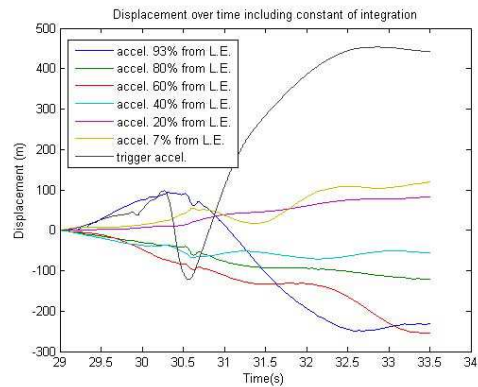


Fig. 11 Integration of the velocity causing drift over time, for run 2.

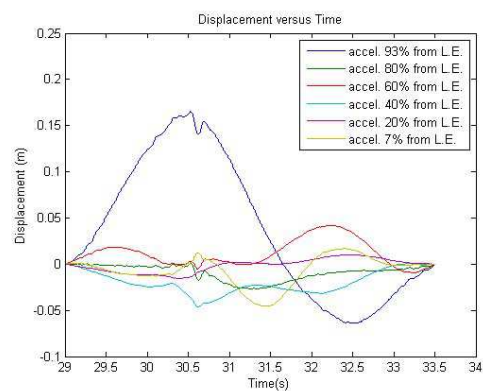


Fig. 12 Integration of the velocity corrected for drift, for run 2.

of the wing there was the issue that 'double taps' of the hammer occurred simply because of the wing springing back before the removal of the impact hammer. This issue is clearly seen when looking at the coherence of the testing, see Figure 15.

The coherence should be close to 1 except near a natural frequency. However, there are large frequency ranges over which the coherence drops to almost 0 away from the natural frequencies of the system. In order to try to improve the readings taken, a different approach was attempted for wing 2. For wing 2, all 6 accelerometers were kept in their original positions and this was coupled with the roving hammer technique. This was done in an attempt to increase the number of consistent readings, thus improve the coherence. However, this approach did not improve

Run	1	2	3	4	5	6
Freestream (m/s)	14.2	11.2	6.4	14.8	10.8	6.1
Maximum gust velocity (m/s)	15.1	11.7	6.9	15.3	11.2	6.3
Minimum gust velocity (m/s)	13.5	10.5	6.0	14.0	10.8	5.7
Gust/Freestream	0.108	0.108	0.152	0.093	0.043	0.101
Max displacement, accel. 6 (m)	0.105	0.165	0.016	0.021	0.105	0.022
Min displacement, accel. 6 (m)	-0.036	-0.064	-0.010	-0.025	-0.036	-0.024

Table 1 Gust input properties and accelerometer displacements for run 2.

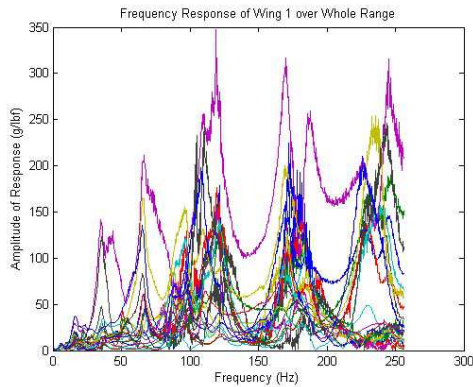


Fig. 13 Response of wing 1 at a range of frequencies.

the coherence, see Figure 16 and the technique used for wing 1 was found to be preferable.

As the frequency responses were not as clear using this technique, only 3 distinct peaks could be observed at 32.3, 37.8 and 92.3Hz, see Figure 17.

For future work, a shaker with a matrix of accelerometers should be considered in order to improve modal testing for the flexible wings.

2.5 Behaviour

A validation methodology was successfully established to determine the level of fidelity of the analytical code. A specific application of the current methods of aeroelastic analysis, both computational and experimental, was used such that the models could be compared to the analytical model like-for-like. Both test methods have used the theory of the typical aeroelastic section to allow for pitch and plunge degrees of freedom for the modelling of a chordwise flexible aerofoil.

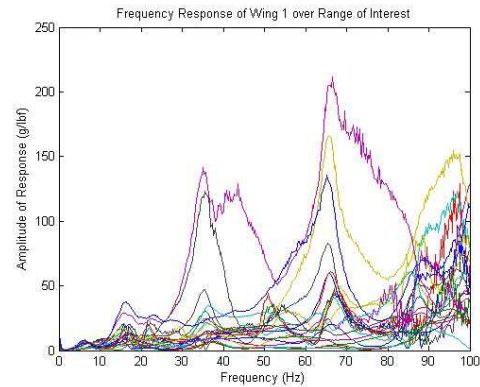


Fig. 14 Response of wing 1 up to 100Hz.

The analytical code can then be further validated by the results arising from the impact hammer testing. The experimental testing could be performed one of the two ways described: by having a roving hammer with a single accelerometer or with multiple accelerometers. From the testing performed, the single accelerometer produced results with a higher level of coherence. This is consistent with information provided by the Aeroelasticity Group at DSTO, who use either a roving hammer or a shaker, rather than a combination, for the reason that the results achieve greater coherence.

3 Finite Element Modelling

A finite element (FE) model was developed in Nastran [10] to replicate the experimental set-up and hence provide a high-fidelity model as an extra source of validation. The model is constructed using 1D elements along the chord and rigid elements along the span. The beam elements are assigned material properties and geo-

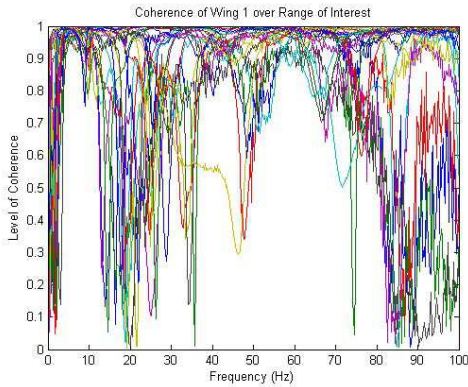


Fig. 15 Coherence plot of wing 1 up to 100Hz.

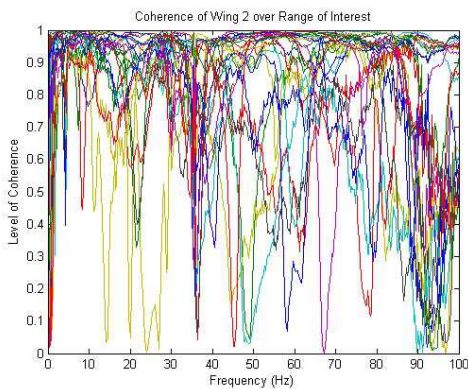


Fig. 16 Coherence plot of wing 2 up to 100Hz.

metric properties as described in section 2. The model is grounded via two springs acting the pitch and plunge degree of freedom. The structural model is presented in figure 18. After performing a normal mode convergence analysis, 15 structural modes are sufficient to achieve an accurate modal convergence. The model is built so

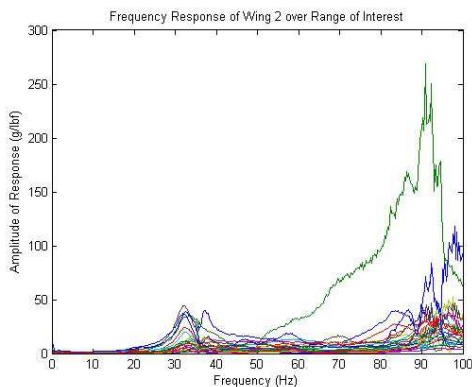


Fig. 17 Response of wing 2 up to 100Hz.

that the aerodynamics is classed as 2D (theoretical infinite span) using the Doublet-Lattice aerodynamics formulation [13]. This is required in order to perform dynamic analysis, in this case verifying the model under gust loads. Initial solution under steady aerodynamic load can be seen in figure 19. The gust generated during the experiment (see figure 20) are used as input in the computational model. The gust is smoothed and re-sampled to avoid computational problems.

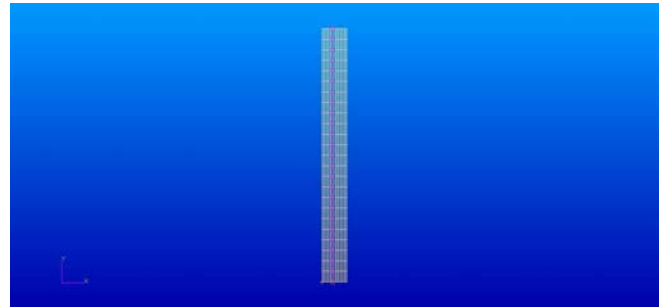


Fig. 18 Finite Element Model

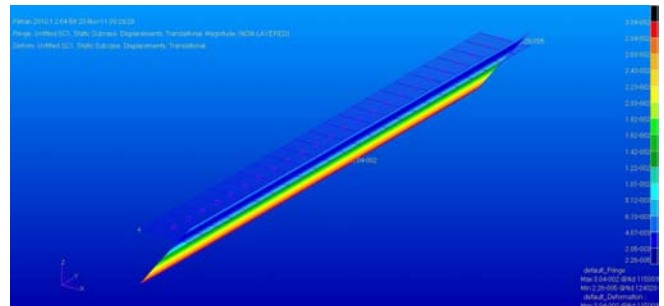


Fig. 19 Finite Element Model under static aerodynamic load

4 Conclusion

A method of experimental testing was established with the test wings, gust generation technique, test rig and experimental setup all taken into account. The method aligns itself in certain ways to Melbourne's work, but allows to a more flexible and portable approach due to having less dependence on the tunnel dimension and access restrictions. Summarised results allow for initial validation, which, when coupled with further experimental testing, will give a wide range of

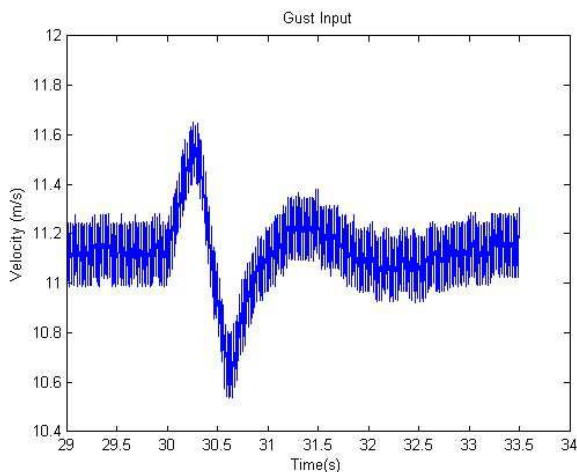


Fig. 20 Experimental Gust Profile

comparison points for the analytical model. The methodology for validation, as well as a range of computational and experimental test cases is provided which could see the validation of a new approach to aeroelastic analysis, which can lead to increased efficiency in the design process. Very little literature exists on experimental, chordwise flexible test wings and thus this paper lays the groundwork for further study. The results from the experimental gust testing make use of repeated gusts to give a wide range of inputs. The gust generation technique is highly successful and repeatable, as it was very easy to replicate one gust after another using the designed test rig.

5 Future Work

The validation of the analytical code will be carried out over the coming months, with the starting point for the comparison being the cases run for this work. Once the level of validity is established, there could be subsequent work on the analytical model or further cases run computationally and experimentally to test a wide range of scenarios. The development of more flexible aerofoils based on the experimental design would give a greater range of results and, again, more results for the validation process. Conducting flow visualisation testing would be suggested for each of these types of wings.

Acknowledgements

The authors would like to acknowledge the support and help of C. Mouser, J. Drobik, H. McCann and T. Mills from DSTO Melbourne.

References

- [1] H.H. Khodaparasta, G. Georgiou, J.E. Cooper, L. Travaglini, S. Ricci, G.A. Vio, and P. Denner. Rapid prediction of worst gust loads. In *52nd Structures, Structural Dynamics, and Material Conference*, 2011.
- [2] T.H.G. Megson. *Aircraft structures for engineering students*. Elsevier/Butterworth Heineemann, London, 2007.
- [3] E. H. Dowell. *A Modern Course in Aeroelasticity*. Kluwer Academic Publishers, 2004.
- [4] G. A. Vio, G. Dimitriadis, J. E. Cooper, K. J. Badcock, M. Woodgate, and A. Rampurawala. Aeroelastic system identification using transonic cfd data for a wing/store configuration. *Aerospace Science and Technology*, 11(2-3):145–154, 2007.
- [5] J. Pederzani and H. Hay-Hairiri. Numerical analysis of heaving flexible airfoils in a viscous flow. *AIAA Journal*, 44(11), 2006.
- [6] A. Postelnicu. A numerical method for flexible airfoils in incompressible inviscid flow. *Acta Mechanica*, 146(1-2), 2001.
- [7] D.-H. Kim, S.-W. Oh, I. Lee, J.-H. Kweon, and J.-H. Choi. Weight optimization of composite flat and curved wings satisfying both flutter and divergence constraints. *Key Engineering Materials*, 334-335:477–480, 2007.
- [8] W. Shyy, H. Aono, S.K. Chimakurthi, P. Trizila, C.-K. Kang, C.E.S. Cesnik, and H. Liu. Recent progress in flapping wing aerodynamics and aeroelasticity. *Progress in Aerospace Sciences*, 46(7):284–327, 2010.
- [9] M. Berci, V. V. Toropov, R. W. Hewson, and P. H. Gaskell. Modelling based on high and low fidelity models interaction for uav gust performance optimisation. In *ASMO UK Conference*, 2008.
- [10] MSC Software Corporation. MSC software, 2011. <http://www.mssoftware.com/>.
- [11] N. Gregory and C. L. O’Reilly. Low-speed aero-

dynamic characteristics of naca0012 aerofoil section, including the effects of upper-surface roughness simulating hoar frost. Reports and Memoranda 3726, Ministry of Defence, Aeronautical research Council, 1973.

- [12] E. D. Jancauskas and W. H. Melbourne. The measurement of aerodynamic admittance using discrete frequency gust generation. *Journal of Wind Engineering and Industrial Aerodynamics*, 23:395–408, 1986.
- [13] W. P. Rodden. *Theoretical and Computational Aeroelasticity*. Chrest Publishing, Camarillo, California, 2011.

6 Spring Data

Translational spring constant = 103.01 N/m

Torsional spring constant = 78.72 N/m

7 Copyright Statement

The authors confirm that they, and/or their company or organization, hold copyright on all of the original material included in this paper. The authors also confirm that they have obtained permission, from the copyright holder of any third party material included in this paper, to publish it as part of their paper. The authors confirm that they give permission, or have obtained permission from the copyright holder of this paper, for the publication and distribution of this paper as part of the ICAS2012 proceedings or as individual off-prints from the proceedings.

Element	Material	Density (g/cm^3)	Young's Modulus (MPa)
Spar	PVC	1.44	3300
Wing 1	Foamex	0.55	1300
Wing 2	PETG	1.27	2050

Table 2 Beam and Wing Materials

Element	Width	Height	Length
Spar	6	6	575
	Chord	Span	Thickness
Wing 1	300	535	2
Wing 2	300	535	1.5

Table 3 Element Dimensions (mm)

Accelerometer	Height on wing	Distance from leading edge
1	250	20
2	250	60
3	250	120
4	250	180
5	250	240
6	250	280

Table 4 Accelerometer Locations (mm)